

## **Motion of a Viscous Fluid Contained in a Cylinder of Infinite Length Subjected to Longitudinal and Torsional Oscillations of Independent Amplitudes**

**Wendell Phillips**

**Karim Rahaman**

Dept. of Mathematics and Statistics  
The University of the West Indies  
St. Augustine, Trinidad, W.I.

### **Abstract**

*The motion of a viscous fluid contained in a cylinder of infinite length subjected to longitudinal and torsional oscillations is investigated. The governing equations are obtained and these are used to derive expressions for the shear stresses and drag forces on the interior wall of the cylinder, as well as the drag coefficient and work done by the drag forces. Graphs are plotted to illustrate the behaviour of the velocity components and other expressions derived in this investigation.*

**Keywords:** Viscous; Longitudinal; Torsional; Cylinder; Oscillations.

### **1. Introduction**

In the year 1990, H. Ramkissoon and S. Majumdar (1990) explored the flow of a viscous fluid in a cylinder of infinite length which was exposed to oscillations of a longitudinal and torsional nature. This was a modified scenario of the original situation which was investigated by M. Casarella and P. Laura (1969), which dealt with obtaining the drag forces developed on the exterior of a circular rod of infinite length immersed in a viscous fluid.

There were many other notable investigators of problems of a similar nature, namely Rajgopal (1983) in the case of a non-Newtonian fluid of second grade, Ramkissoon, Easwaran and Majumdar (1991) in the case of a Polar fluid, Rahaman (2004, 2005) using the situation with an upper-convected Maxwell fluid, and Owen and Rahaman (2006) in the case with an Oldroyd-B fluid. Versions of the problem include the external case with a solid rod of infinite length, the internal case considering a cylinder of infinite length, use of a different type of fluid, oscillations of same frequency, oscillations of different frequencies with same amplitudes, different amplitudes, or any combination of the listed scenarios.

The purpose of this research paper is to explore yet another version of this problem. Here the internal case is examined with the distinction being that this scenario considers oscillations of independent amplitudes, in contrast to other similar problems done in which there was a common parameter defining the amplitudes and hence implying dependence of same.

In this paper the governing equations are obtained and these are used to derive expressions for the shear stresses and drag forces on the interior wall of the cylinder, as well as the drag coefficient and work done by the drag forces. Graphs are plotted to illustrate the behaviour of the velocity components and other expressions derived in this investigation. Some of the results found here are similar to the case done by Ramkissoon and Majumdar (1990).

### **2. Statement and Solution to the Problem**

It is required to find the flow field, the shear stresses, the drag experienced, and the drag coefficient due to the motion of a viscous fluid contained in a cylinder of infinite length of radius  $a$ , subject to longitudinal and torsional oscillations.

Cylindrical coordinates  $(r, \theta, z)$  will be utilized due to the physical nature of the problem, in which the axis of the cylinder coincides with the  $z$ -axis.

It is safe to assume that the torsional and longitudinal oscillations of the cylinder account for the presence of the components  $\hat{\theta}$  and  $\hat{z}$  in the fluid's velocity field. Also, the velocity field  $\underline{q}$  is independent of  $\theta$  since the flow is taken to be axisymmetric. Due to the infinite length of the cylinder, it is reasonable to assume that the fluid's motion is independent of  $z$ . Thus the velocity field  $\underline{q}$  then takes the form

$$\underline{q} = v(r, t)\hat{\theta} + w(r, t)\hat{z} \quad (1)$$

Now a suitable form of the Navier-Stokes equation is

$$\frac{d\underline{q}}{dt} = -\frac{1}{\rho}\nabla p + \nu\nabla^2\underline{q} \quad (2)$$

Expanding (2) gives,

$$\frac{\partial\underline{q}}{\partial t} + (\underline{q} \cdot \nabla)\underline{q} = -\frac{1}{\rho}\nabla p + \nu\nabla^2\underline{q} \quad (3)$$

$\underline{q}$  is a function of  $r$  and time  $t$ , so the term  $\frac{\partial\underline{q}}{\partial t}$  survives in (3).

The continuity equation here is of the form

$$\nabla \cdot \underline{q} = 0 \quad (4)$$

which is automatically satisfied. We shall seek a pressure field which is also independent of  $\theta$  and  $z$ .

The kinematic boundary condition,  $\underline{q}_b$  for the fluid particles at the surface of the cylinder with prescribed velocity,

$$\underline{q}_b = \cos(\Omega t)\hat{e}$$

is that at  $r = a$ ,

$$\underline{q} = \underline{q}_b = \alpha_1 \cos(\Omega t)\hat{\theta} + \alpha_2 \cos(\Omega t)\hat{z} \quad (5)$$

where

$$\hat{e} = \alpha_1 \hat{\theta} + \alpha_2 \hat{z}$$

and  $\Omega, \alpha_1, \alpha_2 \in \mathbb{R}$ , where  $\mathbb{R}$  denotes the set of real numbers.

To obtain a solution of  $\underline{q}$ , substitute (1) into (4) and equate components to get,

$$\hat{r}: \frac{v^2}{r} = \frac{1}{\rho} \frac{\partial p}{\partial r} \quad (6)$$

$$\hat{\theta}: \frac{\partial v}{\partial t} = \nu \left( \frac{\partial^2 v}{\partial r^2} + \frac{1}{r} \frac{\partial v}{\partial r} - \frac{v}{r^2} \right) \quad (7)$$

$$\hat{z}: \frac{\partial w}{\partial t} = \nu \left( \frac{\partial^2 w}{\partial r^2} + \frac{1}{r} \frac{\partial w}{\partial r} \right) \quad (8)$$

### 3. Determination of the Velocity Components

Assume a solution of the form,

$$v(r, t) = \Re(f(r)e^{i\Omega t})$$

where  $\Re$  is the real part. Substituting this in (7) gives the solution as

$$f = \Re \left( AI_1 \left( r \sqrt{i \frac{\Omega}{\nu}} \right) + BK_1 \left( r \sqrt{i \frac{\Omega}{\nu}} \right) \right)$$

where  $I_1$  and  $K_1$  are the modified Bessel's functions of the first and second kind respectively, both of order 1, and A, B are constants to be determined.

Now the velocity field must remain finite and since there exists a singularity of  $K_1(x)$  as  $x$  tends to zero, which corresponds to the axis of the cylinder, then B must be taken to be zero. Using the boundary condition in (5) to determine A gives the  $\hat{\theta}$ -component of the velocity field as,

$$v(r, t) = \mathcal{R} \left( \frac{I_1 \left( r \sqrt{i \frac{\Omega}{\nu}} \right)}{I_1 \left( a \sqrt{i \frac{\Omega}{\nu}} \right)} \alpha_1 e^{i\Omega t} \right) \tag{9}$$

To determine w, assume a solution of the form,  
 $w(r, t) = \mathcal{R}(g(r)e^{i\Omega t})$

Substituting in (8) gives the solution as,

$$g = \mathcal{R} \left( C I_0 \left( r \sqrt{i \frac{\Omega}{\nu}} \right) + D K_0 \left( r \sqrt{i \frac{\Omega}{\nu}} \right) \right)$$

where C and D are constants and  $I_0$  and  $K_0$  are the modified Bessel's functions of the first and second kind respectively, both of order zero.

Now the velocity field must remain finite and since there exists a singularity of  $K_1(x)$  as  $x$  tends to zero, which corresponds to the axis of the cylinder, then D is taken to be zero. Using the boundary condition in (5) to determine C gives the  $\hat{z}$ -component of the velocity field as

$$w(r, t) = \mathcal{R} \left( \frac{I_0 \left( r \sqrt{i \frac{\Omega}{\nu}} \right)}{I_0 \left( a \sqrt{i \frac{\Omega}{\nu}} \right)} \alpha_2 e^{i\Omega t} \right) \tag{10}$$

The velocity components have thus been determined and are given by (9) and (10).

#### 4. Obtaining the Shear Stresses, Drag, Work Done and Drag Coefficient

The shear stresses are given by (Hughes 1979),

$$\tau_{ij} + p\delta_{ij} = 2\mu D_{ij} = \mu(q_{i,j} + q_{j,i})$$

where  $\delta_{ij}$  is the Kronecker delta. In cylindrical coordinates at the boundary of the cylinder, this is

$$\tau_{r\theta} = \mathcal{R} \left( \frac{\sigma\sqrt{i} I_0(\alpha\sqrt{i}) - \frac{2}{a} I_1(\alpha\sqrt{i})}{I_1(\alpha\sqrt{i})} \mu\alpha_1 e^{i\Omega t} \right) \tag{11}$$

where  $\alpha = \sigma a$

and

$$\sigma = \sqrt{\frac{\Omega}{\nu}}$$

$$\tau_{rz} = \mathcal{R} \left( \frac{\sigma\sqrt{i} I_1(\alpha\sqrt{i})}{I_0(\alpha\sqrt{i})} \mu\alpha_2 e^{i\Omega t} \right) \tag{12}$$

The shear stresses have thus been obtained and are given by (11) and (12).

Now the tangential drag  $\underline{D}$  acting per unit length on the cylinder is (Ramkissoon and Majumdar 1990)

$$\underline{D} = -2\pi a [\tau_{r\theta} \hat{\theta} + \tau_{rz} \hat{z}]_{r=a} \tag{13}$$

Substituting (11) and (12) into (13);

$$\underline{D} = -2\pi a \mu \mathcal{R} \left( \left( \frac{\sigma \sqrt{i} I_0(\alpha \sqrt{i}) - \frac{2}{a} I_1(\alpha \sqrt{i})}{I_1(\alpha \sqrt{i})} \alpha_1 \hat{\theta} + \frac{\sigma \sqrt{i} I_1(\alpha \sqrt{i})}{I_0(\alpha \sqrt{i})} \alpha_2 \hat{z} \right) e^{i\Omega t} \right). \quad (14)$$

Now

$$T^2 = \tau_{r\theta}^2 + \tau_{rz}^2,$$

$$\tan \gamma = \frac{\tau_{rz}}{\tau_{r\theta}} \Rightarrow T \cos \gamma = \tau_{r\theta}$$

and

$$T \sin \gamma = \tau_{rz}.$$

Substitute in (13) to get

$$\underline{D} = -2\pi a T \left( (\cos \gamma) \hat{\theta} + (\sin \gamma) \hat{z} \right) = -2\pi a T \hat{\phi} \quad (15)$$

where

$$\hat{\phi} = (\cos \gamma) \hat{\theta} + (\sin \gamma) \hat{z}.$$

Now the work done  $W$  by the drag force  $\underline{D}$  on the fluid per half cycle of motion is (Ramkissoon and Majumdar 1990)

$$W = - \int_0^{\frac{\pi}{\Omega}} \underline{D} \cdot \underline{q}_b dt \quad (16)$$

$$= \pi^2 a \mu \mathcal{R} \left( \left[ \left( \frac{\sigma \sqrt{i} I_0(\alpha \sqrt{i}) - \frac{2}{a} I_1(\alpha \sqrt{i})}{I_1(\alpha \sqrt{i})} \right)^2 \alpha_1^2 + \left( \frac{\sigma \sqrt{i} I_1(\alpha \sqrt{i})}{I_0(\alpha \sqrt{i})} \right)^2 \alpha_2^2 \right]^{\frac{1}{2}} (\alpha_1 \cos \gamma + \alpha_2 \sin \gamma) \right) / \Omega.$$

Now (Ramkissoon and Majumdar 1990)

$$\underline{D}_H = -C q_b^n \hat{e} \quad (17)$$

This is a form of the hypothesized drag force where  $C$  is the drag coefficient.

Substitute (17) into (16) gives,

$$W = - \int_0^{\frac{\pi}{\Omega}} -C q_b^n \hat{e} \cdot \underline{q}_b dt$$

$$= 2\pi a \int_0^{\frac{\pi}{\Omega}} T (\alpha_1 \cos \gamma + \alpha_2 \sin \gamma) \cos(\Omega t) dt$$

$$\Rightarrow C = \frac{2\pi a \int_0^{\frac{\pi}{\Omega}} T (\alpha_1 \cos \gamma + \alpha_2 \sin \gamma) \cos(\Omega t) dt}{\int_0^{\frac{\pi}{\Omega}} q_b^n \hat{e} \cdot \underline{q}_b dt}.$$

It can be shown that

$$q_b^n \hat{e} \cdot \underline{q}_b = \cos^{n+1}(\Omega t) (\alpha_1^2 + \alpha_2^2)^{\frac{n}{2}+1}.$$

Thus one gets,

$C =$

$$\frac{\pi^2 a \mu \mathcal{R} \left( \left[ \left( \frac{\sigma \sqrt{i} I_0(\alpha \sqrt{i}) - \frac{2}{a} I_1(\alpha \sqrt{i})}{I_1(\alpha \sqrt{i})} \right)^2 \alpha_1^2 + \left( \frac{\sigma \sqrt{i} I_1(\alpha \sqrt{i})}{I_0(\alpha \sqrt{i})} \right)^2 \alpha_2^2 \right]^{\frac{1}{2}} (\alpha_1 \cos \gamma + \alpha_2 \sin \gamma) \right)}{(\alpha_1^2 + \alpha_2^2)^{\frac{n}{2}+1} \int_0^{\frac{\pi}{\Omega}} \cos^{n+1}(\Omega t) dt}.$$

### 5. Numerical Analysis

Now the modified Bessel function,  $I$ , can be displayed using the expressions employed by Casarella and Laura (1969) in terms of the moduli and phases of the Kelvin functions (Abramowitz and Stegun 1965). Thus one gets

$$I_0(\sigma r \sqrt{i}) = M_0(\sigma r) e^{i\Theta_0(\sigma r)}$$

$$I_1(\sigma r \sqrt{i}) = -iM_1(\sigma r)e^{i\Theta_1(\sigma r)} \tag{18}$$

where  $M_0, M_1$  and  $\Theta_0, \Theta_1$  are the moduli and phases respectively (Ramkissoon and Majumdar 1990). Substituting (18) into (9), (10), (11) and (12) gives

$$v(r, t) = \mathcal{R} \left( \frac{M_1(\sigma r)}{M_1(\alpha)} e^{i[\Theta_1(\sigma r) - \Theta_1(\alpha)]} \alpha_1 e^{i\Omega t} \right) \tag{19}$$

$$w(r, t) = \mathcal{R} \left( \frac{M_0(\sigma r)}{M_0(\alpha)} e^{i[\Theta_0(\sigma r) - \Theta_0(\alpha)]} \alpha_2 e^{i\Omega t} \right) \tag{20}$$

$$\tau_{r\theta} = \frac{\mu\alpha}{a} \frac{M_0(\alpha)}{M_1(\alpha)} L \alpha_1 \cos(\Omega t + \delta) \tag{21}$$

$$\tau_{rz} = \frac{\mu\alpha}{a} \frac{M_1(\alpha)}{M_0(\alpha)} \alpha_2 \cos(\Omega t + \delta) \tag{22}$$

where

$$L = \left\{ \left\{ \cos \eta - \frac{2 M_1(\alpha)}{\alpha M_0(\alpha)} \right\}^2 + \sin^2 \eta \right\}^{\frac{1}{2}},$$

$$\xi = \Theta_1(\alpha) - \Theta_0(\alpha) - \frac{\pi}{4}.$$

When  $\alpha \gg 1$ , then the asymptotic values in (18) are given by (Abramowitz and Stegun 1965)

$$M_0(\alpha) \approx \frac{e^{\frac{\alpha}{\sqrt{2}}}}{\sqrt{2\pi\alpha}} \left\{ 1 + \frac{1}{8\alpha\sqrt{2}} + \frac{1}{256\alpha^2} + O\left(\frac{1}{\alpha^3}\right) \right\}$$

$$M_1(\alpha) \approx \frac{e^{\frac{\alpha}{\sqrt{2}}}}{\sqrt{2\pi\alpha}} \left\{ 1 - \frac{3}{8\alpha\sqrt{2}} + \frac{9}{256\alpha^2} + O\left(\frac{1}{\alpha^3}\right) \right\}$$

$$\Theta_0(\alpha) \approx \frac{\alpha}{\sqrt{2}} - \frac{\pi}{8} - \frac{1}{8\alpha\sqrt{2}} - \frac{1}{16\alpha^2} + O\left(\frac{1}{\alpha^3}\right)$$

$$\Theta_1(\alpha) \approx \frac{\alpha}{\sqrt{2}} + \frac{3}{8}\pi + \frac{3}{8\alpha\sqrt{2}} + \frac{3}{16\alpha^2} + O\left(\frac{1}{\alpha^3}\right) \tag{23}$$

where  $O$  denotes the order of the succeeding term in brackets.

If we assume that the terms of  $O\left(\frac{1}{\alpha}\right)$  may be neglected, (Ramkissoon and Majumdar 1990) then substituting into (23) gives

$$M_0(\alpha) = M_1(\alpha) \approx \frac{e^{\frac{\alpha}{\sqrt{2}}}}{\sqrt{2\pi\alpha}},$$

$$\Theta_0(\alpha) \approx \frac{\alpha}{\sqrt{2}} - \frac{\pi}{8},$$

$$\Theta_1(\alpha) \approx \frac{\alpha}{\sqrt{2}} + \frac{3}{8}\pi.$$

Thus

$$\eta = \xi = \delta \approx \frac{\pi}{4}$$

$$L \approx 1 \tag{24}$$

Substituting (23) into (20) and (21) gives

$$\begin{aligned} \tau_{r\theta} &\approx \frac{\mu\alpha}{a} \alpha_1 \cos\left(\Omega t + \frac{\pi}{4}\right) \\ \tau_{rz} &\approx \frac{\mu\alpha}{a} \alpha_2 \cos\left(\Omega t + \frac{\pi}{4}\right) \end{aligned} \tag{25}$$

And

$$\tan \gamma = \frac{\tau_{rz}}{\tau_{r\theta}} \approx \frac{\alpha_2}{\alpha_1} \quad (26)$$

Now

$$C = \frac{2\pi a \int_0^{\frac{\pi}{\Omega}} T(\alpha_1 \cos \gamma + \alpha_2 \sin \gamma) \cos(\Omega t) dt}{(\alpha_1^2 + \alpha_2^2)^{\frac{n+1}{2}} \int_0^{\frac{\pi}{\Omega}} \cos^{n+1}(\Omega t) dt} \quad (27)$$

If we assume once again that  $\alpha \gg 1$ , then since

$$T = (\tau_{r\theta}^2 + \tau_{rz}^2)^{\frac{1}{2}},$$

then using (25) and (26) gives

$$T = \frac{\mu\alpha}{a} \cos\left(\Omega t + \frac{\pi}{4}\right) (\alpha_1 L + \alpha_2)^{\frac{1}{2}} \quad (28)$$

Since  $L \approx 1$  then substituting this and (28) into (27) gives

$$C = \frac{2\pi\mu\alpha \int_0^{\frac{\pi}{\Omega}} \cos\left(\Omega t + \frac{\pi}{4}\right) \cos(\Omega t) dt}{(\alpha_1^2 + \alpha_2^2)^{\frac{n-1}{2}} \int_0^{\frac{\pi}{\Omega}} \cos^{n+1}(\Omega t) dt}.$$

The case  $n = 1$  is the only meaningful one where  $C$  is independent of  $\alpha_1$  and  $\alpha_2$  (Ramkissoon and Majumdar 1990). Thus one gets

$$C = \sqrt{2}\pi\mu\alpha$$

and this is the same expression of the drag coefficient obtained when Casarella and Laura (1969) and Ramkissoon and Majumdar (1990) investigated the external and internal problems respectively.

## 6. Graphical Results

From the boundary values given by Casarella and Laura (1969), the selected values are as follows:

$$1 \leq f \leq 10 \text{ Hz}$$

so  $f$  is taken as 5.75 Hz, where  $f = \frac{\Omega}{2\pi}$ . Also (Rambaran and Rahaman 2010),

$$9.30 \times 10^{-7} \leq \nu \leq 1.86 \times 10^{-6} \text{ m}^2 \text{ s}^{-1}.$$

Since the specific gravity of water at 20.2 degrees Celsius is almost 1, the value of  $\nu$  of water at this temperature for all practical purposes is 1.0 centistoke(cst) where

$$1 \text{ cst} = 1 \times 10^{-6} \text{ m}^2 \text{ s}^{-1}.$$

Figures 1 to 4 show the characteristic curves of the  $\hat{\theta}$ -component of the velocity profile for various values of  $\alpha$ .

For the values of  $\Omega t$  taken, it is observed that for  $\alpha$  at 1 and 6,

$$\Omega t = n\pi$$

displays a greater amplitude at the boundary as compared to

$$\Omega t = \frac{2n+1}{2}\pi$$

which displays a smaller amplitude at the boundary, where  $n \in \mathbb{Z}$  and  $\mathbb{Z}$  denotes the set of integers. For the value of  $\alpha$  at 3 and 12, it is noted that the opposite occurs, that is,

$$\Omega t = n\pi$$

displays a smaller amplitude at the boundary while

$$\Omega t = \frac{2n+1}{2}\pi$$

displays a larger amplitude at the boundary. It appears that values of

$$\Omega t = n\pi$$

and values of

$$\Omega t = (n + 1)\pi$$

are symmetric about the vertical axis. The same trend is observed for values of

$$\Omega t = \frac{2n+1}{2}\pi$$

and values of

$$\Omega t = \frac{2n+3}{2}\pi.$$

Across graphs, it is noted that as  $\alpha$  increases, the amplitudes of the oscillations decrease.

Now,

$$\frac{v}{\alpha_1} = \mathcal{R} \left( \frac{I_1(\sqrt{i \cdot 11 \cdot 5\pi})}{I_1(\alpha\sqrt{i})} e^{i\Omega t} \right).$$

The limit as  $\alpha$  tends to infinity of  $\frac{v}{\alpha_1}$  is zero. This indicates that as  $\alpha$  increases then the above approaches the line,

$$\frac{v}{\alpha_1} = 0$$

for various readings of  $\Omega t$ .

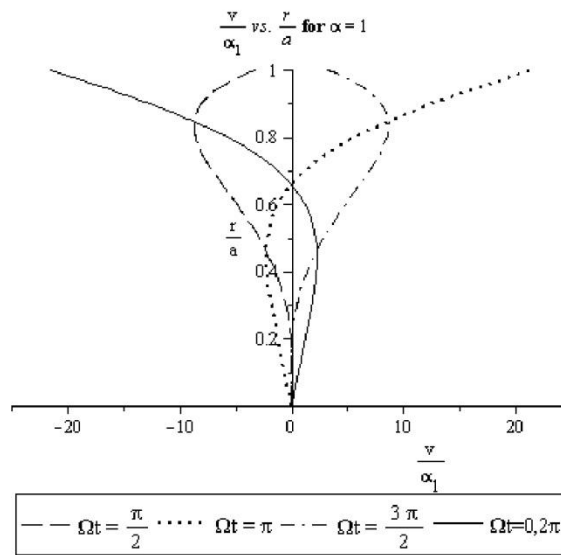


Figure 1:  $\frac{v}{\alpha_1}$  versus  $\frac{r}{a}$  for  $\alpha = 1$

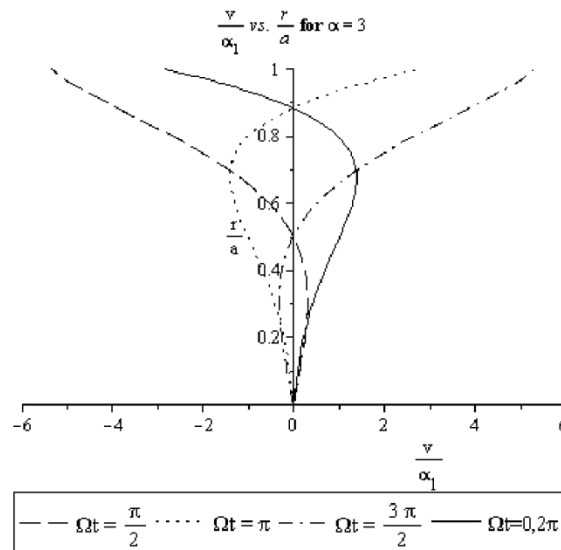


Figure 2:  $\frac{v}{\alpha_1}$  versus  $\frac{r}{a}$  for  $\alpha = 3$

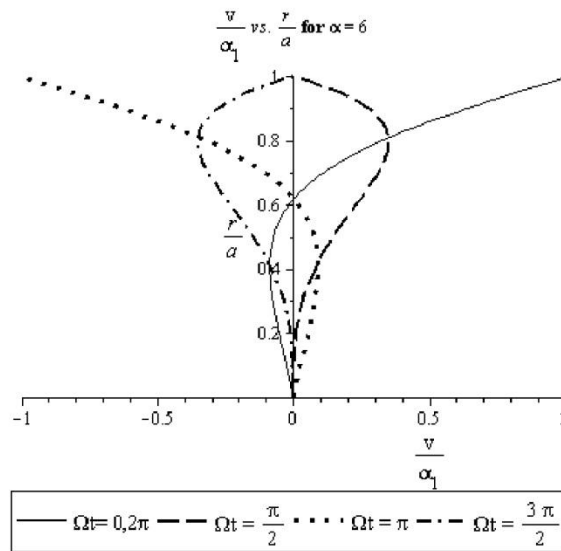


Figure 3:  $\frac{v}{\alpha_1}$  versus  $\frac{r}{a}$  for  $\alpha = 6$

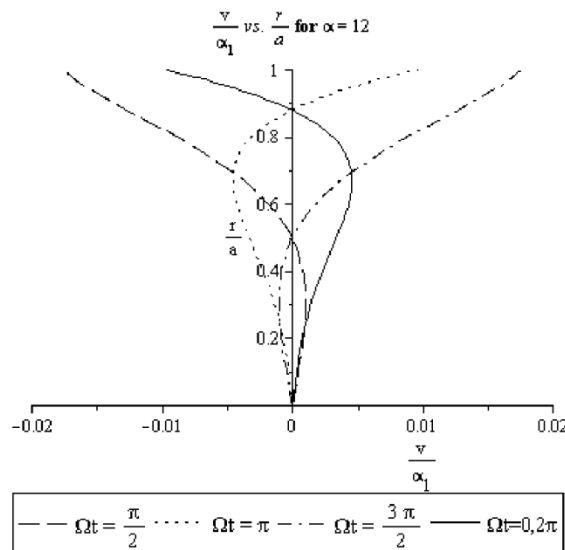


Figure 4:  $\frac{v}{\alpha_1}$  versus  $\frac{r}{a}$  for  $\alpha = 12$

Figures 5 to 8 show the characteristic curves of the  $\hat{z}$ -component of the velocity profile for various values of  $\alpha$ . It is observed that for values of  $\Omega t$  taken and for  $\alpha$  at 1 and 6,

$$\Omega t = \frac{2n+1}{2} \pi$$

experiences a smaller amplitude at the boundary as compared to

$$\Omega t = n\pi$$

which experiences a greater amplitude at the boundary. The opposite case occurs when  $\alpha$  takes values of 3 and 12, where

$$\Omega t = n\pi$$

experiences a smaller amplitude at the boundary and

$$\Omega t = \frac{2n+1}{2} \pi$$

experiences a greater amplitude at the boundary. It appears that values

$$\Omega t = n\pi$$

and values of



$$\Omega t = (n + 1)\pi$$

are symmetric about the vertical axis. The same trend is observed for values of

$$\Omega t = \frac{2n + 1}{2}\pi$$

and values of

$$\Omega t = \frac{2n + 3}{2}\pi$$

Across graphs, it is noted that as  $\alpha$  increases, the amplitudes of oscillations decrease.

Now

$$\frac{w}{\alpha_2} = \mathcal{R} \left( \frac{I_0(\sqrt{i \cdot 11 \cdot 5\pi})}{I_0(\alpha\sqrt{i})} e^{i\Omega t} \right)$$

The limit as  $\alpha$  tends to infinity of  $\frac{w}{\alpha_2}$  is zero. This indicates that as  $\alpha$  increases then the above approaches the line

$$\frac{w}{\alpha_2} = 0$$

for various readings of  $\Omega t$ .

There are various interpretations for an increase in  $\alpha$ . This may mean an increase in frequency of oscillations, an increase in the radius of the cylinder, or a decrease in the viscosity of the fluid. In all cases,  $\alpha$  approaching infinity manifests itself physically as minimum disturbance of the fluid within the cylinder.

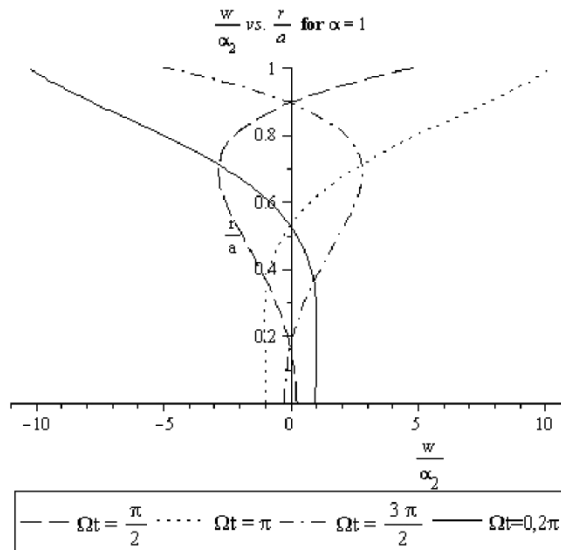


Figure 5:  $\frac{w}{\alpha_2}$  versus  $\frac{r}{a}$  for  $\alpha = 1$

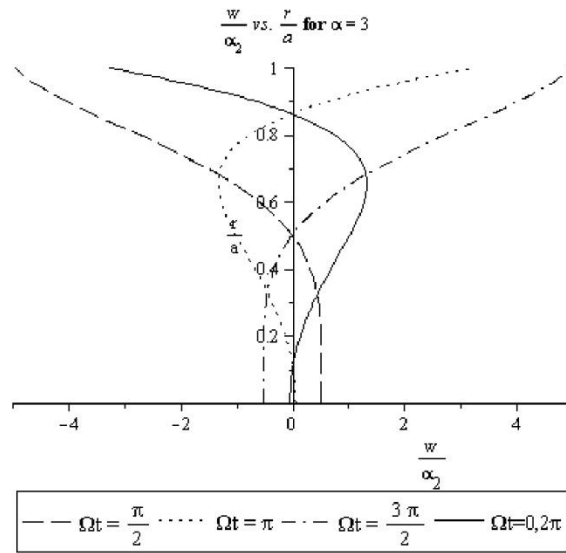


Figure 6:  $\frac{w}{\alpha_2}$  versus  $\frac{r}{a}$  for  $\alpha = 3$

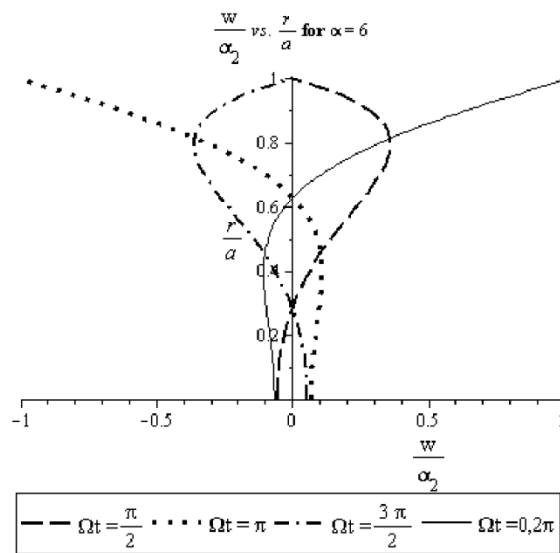


Figure 7:  $\frac{w}{\alpha_2}$  versus  $\frac{r}{a}$  for  $\alpha = 6$

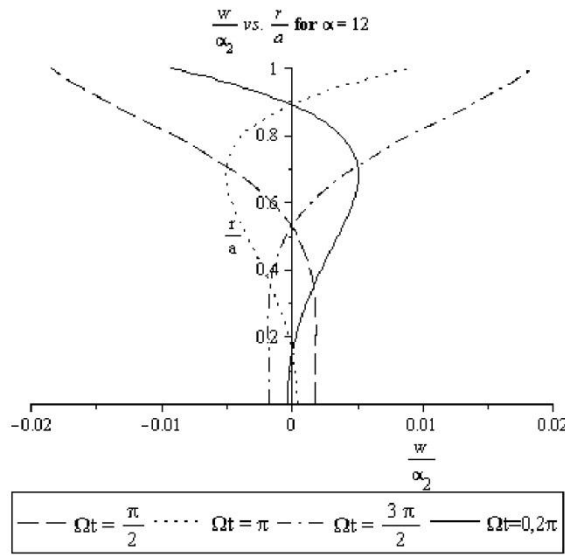


Figure 8:  $\frac{w}{\alpha_2}$  versus  $\frac{r}{a}$  for  $\alpha = 12$

Figures 9 and 10 display the  $\hat{\theta}$  and the  $\hat{z}$ -components of the drag forces against  $\alpha$  respectively for various values of  $\Omega t$ . In both cases there is a generally proportional increase in the drag as  $\alpha$  increases. However, in the first half of the cycle where

$$\Omega t = \frac{\pi}{2} \text{ and } \pi,$$

this increase is observed to occur in one direction, while in the other half of the cycle where

$$\Omega t = 0, 2\pi \text{ and } \frac{3\pi}{2},$$

this proportional increase is observed to occur in the opposite direction. It appears that values of

$$\Omega t = n\pi$$

and values of

$$\Omega t = (n + 1)\pi$$

are symmetric about the horizontal axis. The same trend is observed for values of

$$\Omega t = \frac{2n+1}{2}\pi$$

and values of

$$\Omega t = \frac{2n+3}{2}\pi.$$

For these graphs, it is observed that for values of

$$\Omega t = \frac{2n+1}{2}\pi$$

the drag is of a greater magnitude, as compared to corresponding values of

$$\Omega t = (n + 1)\pi$$

where the drag is of a smaller magnitude.

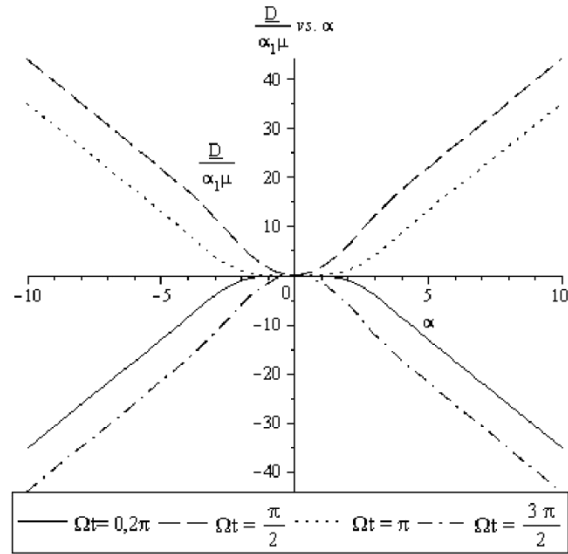


Figure 9:  $\hat{\theta}$ -component of  $\frac{D}{\alpha_1 \mu}$  versus  $\alpha$

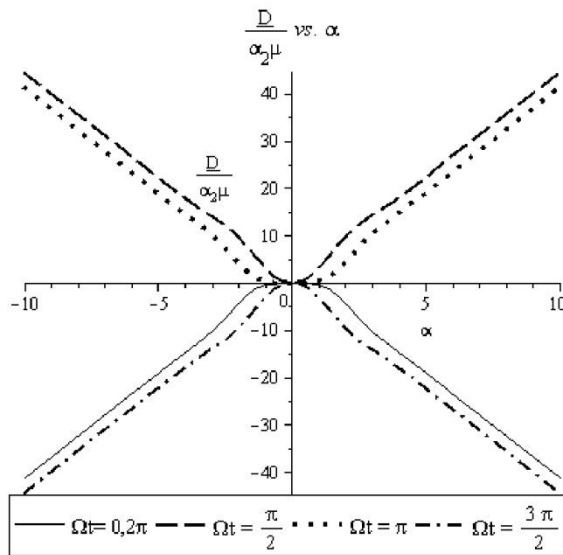


Figure 10:  $\hat{z}$ -component of  $\frac{D}{\alpha_2 \mu}$  versus  $\alpha$

Figure 11 shows the characteristic curves of the  $\hat{\theta}$ - component of the dragforces plotted against  $\Omega t$  for various values of  $\alpha$ . It can be seen from these plots that while the periods of oscillation remain the same for different values of  $\alpha$ , the amplitudes increase as  $\alpha$  increases. The same behaviour is observed for the  $\hat{z}$ -component of the drag forces plotted against  $\Omega t$  in figure 12.

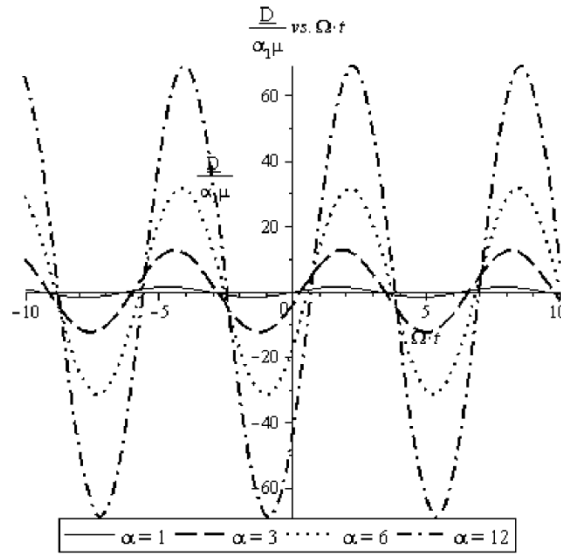


Figure 11:  $\hat{\theta}$ -component of  $\frac{D}{\alpha_1\mu}$  versus  $\Omega t$

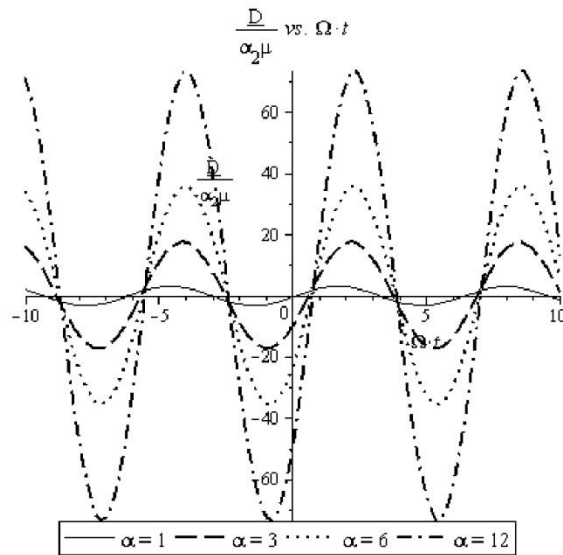


Figure 12:  $\hat{z}$ -component of  $\frac{D}{\alpha_2\mu}$  versus  $\Omega t$

Figure 13 represents the work done against  $\alpha$  for various ratios of amplitudes. It can be seen from the characteristics that with a low ratio of  $\frac{\alpha_1}{\alpha_2}$  there is a gentle increase in work done. However, as this ratio of  $\frac{\alpha_1}{\alpha_2}$  increases, the amount of work done becomes much greater. As  $\alpha$  increases, the magnitude of work done also increases.

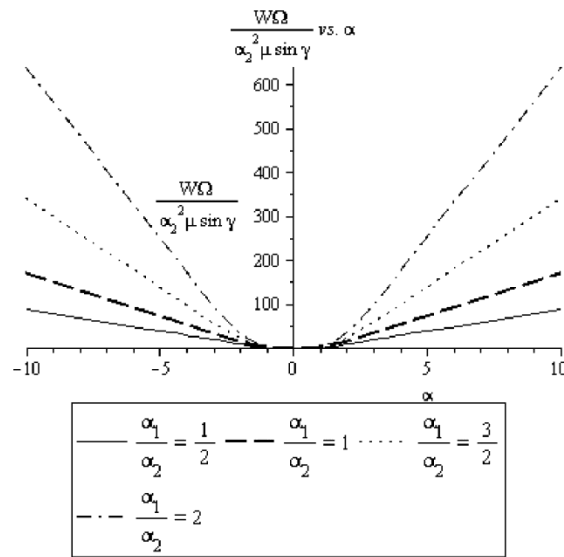


Figure 13:  $\hat{z}$ -component of  $\frac{W\Omega}{\alpha_2^2 \mu \sin \gamma}$  versus  $\alpha$

**References**

Abramowitz, M. and I.A. Stegun 1965. *Handbook of Mathematical functions*. New York. Dover Publ. Inc.

Casarella, M.J. and P.A. Laura 1969. Drag on an Oscillating Rod with Longitudinal and Torsional Motion. *Journal of Hydronautics* 3 (4): 180-183.

Hughes, William F. 1979. *An Introduction to Viscous Flow*. New York. Hemisphere Publishing Corporation.

Owen, D. and K. Rahaman 2006. On the Flow of an Oldroyd-B Liquid through a Straight Circular Tube performing Longitudinal and Torsional Oscillations of Different Frequencies. *Mathematicas: Enseñanza Universitaria* 14 (1): 35-43.

Rahaman, K. 2004. Internal Flow Due to the Longitudinal and Torsional Oscillation of a Cylinder. *Asian Journal of Information Technology* 3 (10): 960-966.

Rahaman, K. 2005. Non-Newtonian Flow Due to a Solid Oscillating Rod. *Asian Journal of Information Technology* 4 (2): 243-249.

Rajgopal, K.R. 1983. Longitudinal and Torsional Oscillations of a Rod in a Non-Newtonian Fluid. *Acta Mechanica* 49:281-285.

Rambaran, A., and K. Rahaman 2010. General Newtonian Flow Due to the Longitudinal and Torsional Oscillation of a Rod. *Journal of Engineering and Applied Sciences* 5 (1): 19-29.

Ramkissoon, H. and S.R. Majumdar 1990. Flow Due to the Longitudinal and Torsional Oscillation of a Cylinder. *Journal of Applied Mathematics and Physics (ZAMP)* 41:598-603.

Ramkissoon, H., C.V. Easwaran, and S.R. Majumdar, 1991. Longitudinal and Torsional Oscillation of a Rod in a Polar Fluid. *International Journal of Engineering Sciences* 29 (2): 215-221.

Watson, G.N. 1952. *Theory of Bessel Functions*. Ann Arbor, Michigan. Syndics of the Cambridge University Press.